Phyton-
International Journal of
Experimental Botany

Tech Science Press

http://doi.org/10.32604/phyton.2026.076015

ARTICLE

Investigation on Chemical Constituents from *Prunus cerasifera* Ehrh. Fruits and Evaluation of Their Anti-Inflammatory Activity

Haofan Lv[1], Qihang Zhang[1], Yufan He[1], Wuwei Xin[2], Wei Liu[1,*] and Chunpeng Wan[1,3,*]

[1]University and College Key Lab of Natural Product Chemistry and Application in Xinjiang, School of Chemistry and Chemical Engineering, Yili Normal University, Yining, China
[2]Xinjiang Tianhongrun Biotechnology Co., Ltd., Changji, China
[3]Jiangxi Key Laboratory for Postharvest Technology and Nondestructive Testing of Fruits and Vegetables, College of Agronomy, Jiangxi Agricultural University, Nanchang, China
*Corresponding Authors: Wei Liu. Email: ucasliuwei@126.com; Chunpeng Wan. Email: chunpengwan@jxau.edu.cn

Received: 12 November 2025; Accepted: 13 March 2026; Published: 28 April 2026

ABSTRACT: The fruits of *Prunus cerasifera* Ehrh. have been traditionally utilized as both medicinal and edible resource, however, their specific phytochemical profile and anti-inflammatory mechanisms remain to be fully elucidated. This study aimed to isolate and identify the chemical constituents from the fruits and evaluate their anti-inflammatory activities. The separation was performed using a combination of chromatographic techniques. The structures of the obtained compounds were elucidated using a combination of ^{1}H and ^{13}C nuclear magnetic resonance (NMR) and electrospray ionization mass spectrometry (ESI-MS). The anti-inflammatory activity of the compounds was initially investigated based on their capacity to inhibit nitric oxide (NO) release from lipopolysaccharide (LPS)-stimulated RAW264.7 macrophages and further validated in a zebrafish inflammatory model. The results indicated that eight compounds were successfully isolated from *Prunus cerasifera* Ehrh. fruits for the first time, including ursolic acid (**1**), corosolic acid (**2**), oleanolic acid (**3**), maslinic acid (**4**), 2-*O*-(3′,4′-dihydroxybenzoyl)-2,4,6-trihydroxyphenylacetic acid (**5**), neochlorogenic acid (**6**), chlorogenic acid (**7**), 3-*O*-*p*-coumaroylquinic acid (8). In the LPS-induced RAW264.7 cell model, compounds **6** and **7** exhibited stronger activity than the positive control dexamethasone (Dex, IC_{50} = 11.13 μM ± 0.43 μM), with IC_{50} values of 6.33 μM ± 0.18 μM and 8.06 μM ± 0.35 μM, respectively. In the LPS-induced zebrafish inflammation model, compounds **6** and **7** again demonstrated significant efficacy, exerting their anti-inflammatory effect primarily through the modulation of pro-inflammatory factors Interleukin-6 (IL-6) and Interleukin-1β (IL-1β).

KEYWORDS: *Prunus cerasifera* Ehrh.; triterpenoids; phenolic acids; anti-inflammatory

1 Introduction

Inflammation serves as a cardinal host defense mechanism against by endogenous and exogenous stimuli such as infection, trauma, or toxic compounds [1,2]. In the past several years, the role of inflammation in the onset and progression of numerous diseases has attracted growing interest, making it a focal point in modern medical research. Current clinical anti-inflammatory strategies mainly include nonsteroidal anti-inflammatory drugs, glucocorticoids and biologics [3]. While these agents have demonstrated certain therapeutic efficacy, their side effects and limitations remain a concern. Therefore, developing novel anti-inflammatory drugs derived from natural sources has become an important direction in pharmaceutical research.

Prunus cerasifera Ehrh. is a species of the genus *Prunus* in the Rosaceae family. Native to parts of Asia and Eastern Europe, its distribution within Asia is primarily concentrated in Huocheng area, Xinjiang Uygur Autonomous Region, China [4,5]. *Prunus cerasifera* Ehrh. fruits were reported to have abundant primary metabolites such as organic acids, vitamins and polysaccharides, as well as secondary metabolites including phenolic and terpenoid compounds. These constituents possess anti-inflammatory, antioxidant, and antitumor properties [6,7]. For instance, Hooshmand et al. extracted polyphenols from dried plum and conducted activity studies, finding that they possessed anti-inflammatory and antioxidant properties [8]. Separately, Duan et al. applied liquid chromatography-tandem mass spectrometry (LC-MS/MS) and network pharmacology to profile *Prunus cerasifera*, identified phenolic acids and flavonoids as its main constituents and found its anti-inflammatory effects were linked to the tumor necrosis factor-alpha (TNF-α) signaling pathway, inflammatory cytokines and the mitogen-activated protein kinase (MAPK) pathway [9]. However, the literature data on the isolation of active compounds from *Prunus cerasifera* Ehrh. fruits and the comprehensive evaluation of their anti-inflammatory activity are relatively limited. Therefore, this study used the fruits of *Prunus cerasifera* Ehrh., isolated eight different compounds through various chromatographic methods (Fig. 1), and assessed their anti-inflammatory activity in both *in vitro* cellular and *in vivo* zebrafish models.

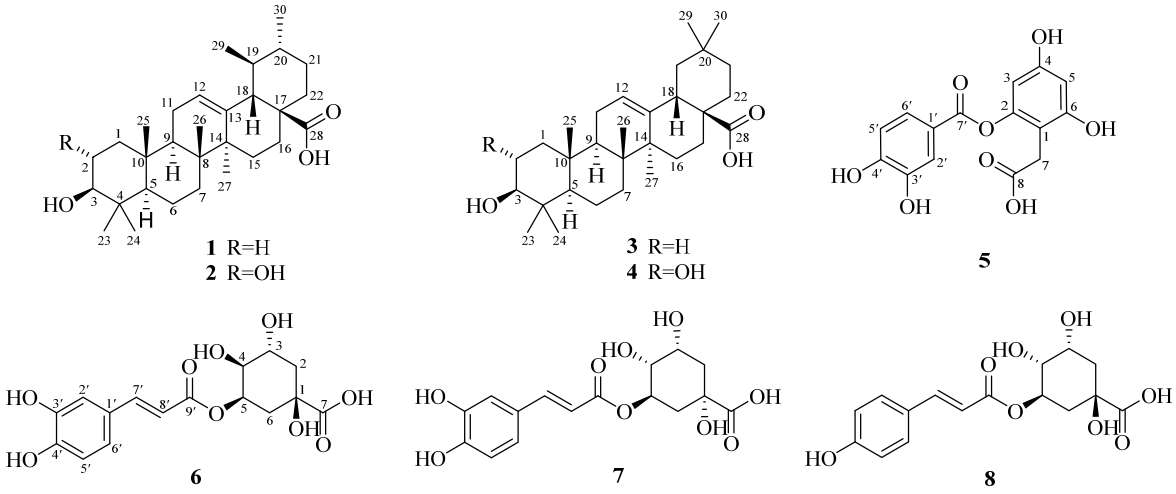

Figure 1: Structures of compounds **1**–**8** from *Prunus cerasifera* Ehrh. fruits.

2 Experimental Section

2.1 Routine Experimental Techniques

The ^{1}H and ^{13}C NMR (Agilent DD2 600 MHz, Santa Clara, CA, USA) spectra were acquired by using tetramethylsilane (TMS) as the internal standard. The semi-preparative high-performance liquid chromatography (HPLC) instrument used in this study was equipped with a Thermo Scientific UltiMate 3000 DGLC system, a VH-D20-A pump and a diode array detector (DAD). A Thermo Scientific Accucore C18 analytical column (0.75 mL/min, 2.6 μm, 2.1 mm × 150 mm; Thermo-Fisher Scientific, USA) was employed for analysis, and a Shim-pack Scepter HD-C18-80 column (3 mL/min, 5 μm, 10.0 mm × 250 mm; Shimadzu, Kyoto, Japan) was used for preparative. ESI-MS analysis was performed in positive ion mode using a Waters Acquity QDa single quadrupole mass spectrometer equipped with an ESI source (Waters, Milford, MA, USA). The Infinite F50 microplate reader was used to measure the absorbance (Tecan, Männedorf, Switzerland). Normal-phase silica gel (300 mesh-400 mesh, UniSil, Nanomicro, Suzhou, China), middle chromatogram

isolated gel (MCI gel) (CHP20P, Supelco, USA), octadecylsilyl (ODS) gel (YMC, Japan), Sephadex LH-20 (Cytiva, Uppsala, Sweden) and D101 macroporous adsorption resin (Haiguang Chemical Co., Ltd., Tianjin, China) were used as stationary phases for column chromatographic separation. All solvents were either HPLC-grade (LiChrosolv, Merck, Germany) or analytical-grade purchased from local suppliers (Tansoole, Shanghai, China). IL-6 and IL-1β enzyme-linked immunosorbent assay (ELISA) kits were obtained from Shanghai Yuanxin Biotechnology Co., Ltd. (Shanghai, China).

2.2 Plant Materials

The fruits of *Prunus cerasifera* Ehrh. used in this study were collected in August 2024 from Huocheng County, Ili Prefecture, Xinjiang, China. The plant material was authenticated by Professor Yang Xiaorong of the School of Biological Science and Technology, Ili Normal University. The samples are stored at −80°C in the College of Chemistry and Chemical Engineering of the same university.

2.3 Extraction and Isolation Procedure

Fresh *Prunus cerasifera* Ehrh. fruits (10.0 kg) were deseeded and macerated at room temperature in three batches, each using 20 L of MeOH for 7 days. The crude extract (106.3 g) was acquired by concentration of the combined extracts under reduced pressure. Water was used to suspend the resulting material and it was extracted continuously with petroleum ether, ethyl acetate, and n-butanol. The respective fractions were concentrated to yield the petroleum ether (PE) (15.7 g), ethyl acetate (EA) (38.9 g), n-butanol (24.3 g), and aqueous (22.8 g) fractions. The EA fraction (38.5 g) was separated by D101 macroporous resin column chromatography (EtOH-H_2O, 20:100–100:0), chromatographic separation was carried out using a solvent gradient, affording five fractions (Fr.A–Fr.E). Separation of Fr.A (8.6 g) by MCI column chromatography (MeOH-H_2O, 10:90–100:0), chromatographic separation was carried out using a solvent gradient, affording five subfractions (Fr.A1–Fr.A5). Purification of Fr.A1 (2.1 g) using Sephadex LH-20 gel column chromatography (MeOH–H_2O, 20:80) yielded four subfractions (Fr. A1a–Fr. A1d). Purification of Fr. A1c (123.3 mg) by semi-preparative HPLC using a MeOH-H_2O gradient (0–20 min, 28:72–28:72; 20–23 min, 28:72–100:0; 23–26 min, 100:0–100:0, 3 mL/min) yielded compounds **6** (34.3 mg, t_R = 9.0 min), **7** (44.3 mg, t_R = 16.2 min), and **8** (20.2 mg, t_R = 13.7 min). Separation of Fr.B (4.4 g) using silica gel column chromatography, with a DCM-MeOH gradient (50:1–1:1) afforded nine subfractions (Fr.B1–Fr.B9). Fr.B1 (851.8 mg) was separated by ODS column chromatography, with elution performed using a MeOH-H_2O gradient (15:85–100:0) to obtain six subfractions (Fr. B1a–Fr. B1f). Purification of Fr. B1b (103.0 mg) by semi-preparative HPLC (16% MeOH-H_2O, 3 mL/min) obtained compound **5** (8.9 mg, t_R = 16.2 min). Separation of Fr.D (4.2 g) using silica gel column chromatography, with a PE-EA gradient (7:1–1:1) yielded six subfractions (Fr.D1–Fr.D6). Separation of Fr.D3 (339.1 mg) by Sephadex LH-20 gel column chromatography (80% MeOH-H_2O) yielded four subfractions (Fr. D3a–Fr. D3e). Purification of Fr.D3b (93.0 mg) by semi-preparative HPLC (89% MeOH-H_2O, 3 mL/min) afforded compounds **1** (18.8 mg, t_R = 18.8 min) and **3** (20.0 mg, t_R = 17.4 min). Finally, separation of Fr.E (3.4 g) by silica gel column chromatography, with a PE-EA gradient as the mobile phase (20:1–1:1) obtained five subfractions (Fr.E1–Fr.E5). Purification of Fr.E1 (324.1 mg) by semi-preparative HPLC (93% MeOH-H_2O, 3 mL/min) yielded compounds **2** (25.0 mg, t_R = 37.9 min) and **4** (23.0 mg, t_R = 38.8 min).

2.4 In Vitro Anti-Inflammatory Activity Assay

RAW264.7 cells were maintained under standard culture conditions in high-glucose Dulbecco's modified Eagle medium (DMEM) containing 10% fetal bovine serum (FBS) and 1% penicillin-streptomycin. Treatment

of cells with 2.0 μg/mL LPS was used to induce stimulation. All test compounds were initially dissolved in dimethyl sulfoxide (DMSO) and subsequently diluted in complete DMEM for treatment.

The cytotoxicity of compounds **1**–**8** was assessed according to the procedure described in reference [10]. Briefly, RAW264.7 cells were seeded in 96-well plates at a density of 2.0×10^4 cells per well and incubated for 24 h. After this period, cells were treated with the test compounds (**1**–**8**) by replacing the medium with 100 μL of serum-free DMEM, then incubated for another 24 h. Subsequently, the cytotoxicity of the compounds was evaluated using the CCK-8 assay according to the instruction manual. Specifically, the medium in each well was exchanged for 100 μL of a mixture of CCK-8 reagent and fresh DMEM (at a 1:9 ratio). The plate underwent a 2 h, light-protected incubation before absorbance measurement at 450 nm. The cell viability (V) was calculated according to Eq. (1). In the equation, A_0, A_1 and A_2 denote the absorbance values for the blank group, the control group, and the sample group, respectively.

$$V = [(A_2 - A_0)/(A_1 - A_0)] \times 100\% \quad (1)$$

To evaluate the anti-inflammatory activity of compounds **3**–**8**, the NO content in RAW264.7 cells was measured using a nitric oxide assay kit according to the procedure described in reference [11]. Briefly, following a 24 h incubation after seeding at 2.0×10^4 cells/well in 96-well plates, RAW264.7 cells were treated with test compounds (5, 10, 20, and 40 μM) or the positive control Dex in fresh medium, respectively. The cells were cultured for 2 h before being stimulated with LPS (2.0 μg/mL) for 24 h. Subsequently, 50 μL aliquots of the supernatant were mixed with an equal volume of a freshly prepared 1:1 mixture of Griess reagents I and II, followed by absorbance measurement at 540 nm. The IC_{50} values were determined using GraphPad Prism 8.0 software.

2.5 In Vivo Anti-Inflammatory Activity Assay

The anti-inflammatory activity of compounds **6** and **7** was further evaluated according to the procedure described in the reference [12]. Tg (lyz:EGFP)/Tg (mpeg1:EGFP) strain zebrafish were reared under controlled conditions (28°C ± 0.5°C, pH = 6.8 ± 0.5, 14 h/10 h light/dark cycle). Mature and healthy adult fish were selected (female:male = 1:2) and acclimated for 24 h in breeding tanks with divider. Upon removal of the divider, spawning was induced by light stimulation. Fertilized eggs collected within 1 h–3 h were rinsed with 3 × E3 embryo medium and subsequently incubated at 28°C ± 0.5°C for standardized development.

Zebrafish larvae were placed into a 24-well plate at a density of 30 larvae per well. Inflammation was induced by treatment with 1 μg/mL LPS, followed by incubation with either the positive control Dex or compounds **6** and **7** at gradient concentrations (60, 40, and 20 μM) for 2 h. After treatment, larvae were homogenized in ice-cold phosphate-buffered saline (PBS) (0.01 M, pH = 7.4) at a 1:9 (w/v) ratio. The homogenate was centrifuged at low temperature, and the levels of IL-1β and IL-6 in the supernatant were measured using specific ELISA kits according to the manufacturer's instructions.

2.6 Statistical Calculations

To ensure the reliability of the results, all experimental data were derived from three independent experimental replicates, data are expressed as mean ± standard deviation (SD), $^{*}p < 0.05$, $^{**}p < 0.01$, $^{***}p < 0.001$, $^{****}p < 0.0001$, $^{ns}p \geq 0.05$ vs. control group. In addition, IC_{50} values were determined by nonlinear regression analysis using GraphPad Prism 8.0 software.

3 Result

3.1 Structural Elucidation

Compound **1** was acquired as a white amorphous powder. The ^{13}C NMR data, combined with the ESI-MS signal at m/z 479.35 for $[M + Na]^+$ (calculated for $C_{30}H_{48}O_3$, 479.35), allowed for the assignment of the molecular formula as $C_{30}H_{48}O_3$. Detailed analysis of the ^{1}H NMR spectrum (Fig. S1) revealed seven methyl signals at δ_H 1.13 (3H, s, H_3-27), 0.98 (6H, s, H_3-23/29), 0.97 (3H, s, H_3-26), 0.90 (3H, d, J = 6.5 Hz, H_3-30), 0.86 (3H, s, H_3-24), and 0.79 (3H, s, H_3-25). Additionally, the existence of a double bond was revealed by an olefinic proton signal at δ_H 5.24 (1H, t, H-12), this inference was further corroborated by the corresponding ^{13}C NMR signals for the olefinic carbons at δ_C 139.6 (C-13) and 126.9 (C-12). The ^{13}C NMR spectrum (Fig. S2) displayed 30 carbon signals. A carbonyl group was identified by the downfield signal at δ_C 181.7 (C-28), while an oxygenated carbon was indicated by the signal at δ_C 79.7 (C-3). Based on these characteristic features, compound **1** was preliminarily identified as a triterpenoid. Through systematic comparison of the spectroscopic data (Table 1) with the data reported, compound **1** was confirmed as ursolic acid [13].

Compound **2** was yielded as a white amorphous powder. An ESI-MS ion at m/z 495.35 $[M + Na]^+$ (calculated for $C_{30}H_{48}O_4Na$, 495.35), along with ^{13}C NMR data, established the molecular formula as $C_{30}H_{48}O_4$. A comparative analysis of the ^{1}H and ^{13}C NMR spectra of compounds **2** and **1** (Figs. S1–S4) showed them to be highly similar, suggesting that both compounds share the same skeletal structure. However, the ^{13}C NMR spectrum of compound **2** showed two oxygenated carbon signals at δ_C 84.5 (C-3) and 69.5 (C-2), as compared to a single oxygenated carbon signal at δ_C 79.7 (C-3) in compound **1**, indicating the location of an additional hydroxyl group at C-2 in compound **2**. The downfield shift of C-3 from δ_C 79.7 to 84.5 further supported the presence of a vicinal diol system. Contrast the spectroscopic data (Table 1) in detail with the data published identified 2 as corosolic acid [14].

Table 1: The ^{13}C NMR data of compounds **1**–**4** (δ in ppm).

No	1	2	3	4	No	1	2	3	4
1	38.1	48.3	39.8	48.1	16	25.3	25.3	24.1	24.6
2	27.9	69.5	27.9	69.5	17	48.0	49.1	47.8	47.7
3	79.7	84.5	79.7	84.5	18	54.4	54.4	42.7	42.8
4	39.0	40.8	39.8	40.6	19	40.0	40.4	47.3	47.3
5	56.7	56.7	56.8	56.7	20	39.8	40.4	31.6	31.6
6	19.5	19.5	19.5	19.6	21	31.8	31.8	34.9	34.9
7	34.3	34.2	34.0	33.9	22	37.1	38.1	33.8	33.9
8	40.8	40.5	40.6	40.5	23	28.8	29.3	28.7	29.3
9	48.0	48.3	49.0	49.2	24	16.0	17.6	16.3	17.8
10	40.4	39.2	38.2	39.3	25	16.4	17.8	15.9	17.1
11	24.4	24.4	24.5	24.1	26	17.8	17.2	17.7	17.5
12	126.9	126.7	123.6	123.4	27	24.1	24.1	26.4	26.4
13	139.6	139.8	145.2	145.4	28	181.7	181.7	181.9	180.8
14	43.3	43.3	42.9	42.9	29	17.7	17.5	33.4	33.6
15	29.2	29.2	28.8	28.8	30	21.6	21.6	24.0	24.0

Compounds **1**–**4** tested in CD_3OD, 100 MHz.

Compound **3**, a white amorphous powder. The presence of seven singlet methyl signals was evident from the ^{1}H NMR spectrum (Fig. S5): δ_H 1.17 (3H, s, H_3-30), 0.99 (3H, s, H_3-29), 0.96 (6H, s, H_3-26/27), 0.92 (3H, s, H_3-25), 0.83 (3H, s, H_3-24), and 0.79 (3H, s, H_3-23), along with one olefinic proton at δ_H 5.25 (1H, s, H-12). The ^{13}C NMR spectrum displayed 26 carbon signals (Fig. S6), among which the resonances

at δ_C 145.2 (C-13) and 123.6 (C-12) were indicative of a double bond, while the signal at δ_C 79.7 (C-3) was characteristic of an oxygenated carbon. Contrasting the spectroscopic data (Table 1) with previously published data showed that it was highly similar to oleanolic acid [13]. However, the ^{13}C NMR spectrum (Fig. S6) showed no distinct signal for the carbonyl carbon signal (C-28). To further confirm the identity of compound **3**, it was co-chromatographed with an oleanolic acid standard by HPLC using a MeOH-H_2O gradient (0–25 min, 75:25–100:0; 25–30 min, 100:0–100:0) at a flow rate of 0.75 mL/min. The results showed that the retention times of the two were identical. Additionally, the molecular formula $C_{30}H_{48}O_3$ was determined based on ESI-MS data, as evidenced by the $[M - H]^+$ ion at m/z 455.35 (calculated for $C_{30}H_{47}O_3$, 455.35). Based on the comprehensive spectroscopic analysis and comparison with authentic standard, compound **3** was conclusively identified as oleanolic acid [13].

Compound **4**, a white amorphous powder. The ^{13}C NMR data, combined with the ESI-MS signal at m/z 495.34 for $[M + Na]^+$ (calculated for $C_{30}H_{48}O_4Na$, 479.35), allowed for the assignment of the molecular formula as $C_{30}H_{48}O_4Na$. ^{1}H and ^{13}C NMR spectroscopic analysis revealed that compound **4** shared structural similarity with compound **3** (Figs. S6–S8), both possessing a triterpenoid skeleton. A key distinction was the presence of two oxygenated carbon signals in the downfield region of compound **4** [δ_C 84.5 (C-3) and 69.5 (C-2)] (Table 1), whereas compound **3** displayed only one at δ_C 79.7 (C-3). This suggested that compound **4** is a hydroxylated derivative of oleanolic acid. Comparison of its ^{1}H and ^{13}C NMR data with those reported for maslinic acid [14] revealed high similarity. However, the absence of the carboxylic acid carbonyl signal was noted in the ^{13}C NMR spectrum of compound **4**. Therefore, compound **4** was co-chromatographed with an authentic maslinic acid standard by HPLC using a MeOH-H_2O gradient (0–25 min, 75:25–100:0; 25–30 min, 100:0–100:0) at a flow rate of 0.75 mL/min, and the retention time of compound **4** was identical to that of the standard. Additionally, mass spectrometric analysis provided further supporting evidence. Based on these results, compound **4** was unequivocally identified as maslinic acid.

Compound **5** was acquired as a white amorphous powder. The presence of the $[M + H]^+$ ion at m/z 321.06 (calculated for $C_{15}H_{13}O_8$, 321.06) in the ESI-MS spectrum established the molecular formula as $C_{15}H_{12}O_8$. The presence of five olefinic protons was evident from the ^{1}H NMR spectrum (Fig. S9): δ_H 7.55 (2H, br s, H-4/8), 6.86 (1H, s, H-6), 6.25 (1H, s, H-3), and 6.14 (1H, s, H-5). In the ^{13}C NMR spectrum (Fig. S10), fourteen carbon signals were detected in the downfield region. These carbonyl signals were assigned to a carboxyl group δ_C 177.1 (C-8) and an ester carbonyl δ_C 166.5 (C-7′), respectively. The remaining twelve sp^2-hybridized carbons were observed at δ_C 158.6 (C-4), 158.3 (C-2), 152.4 (C-4′), 152.2 (C-6), 146.4 (C-3′), 124.4 (C-6′), 121.7 (C-1′), 117.9 (C-2′), 116.1 (C-5′), 108.1 (C-1), 102.1 (C-5), and 101.4 (C-3). The presence of five aromatic protons and ten sp^2-hybridized carbons strongly suggested the existence of two polysubstituted benzene rings in the molecule. Based on systematic analysis of the spectroscopic data (Table 2) and comparison with literature values, compound **5** was identified as 2-O-(3′,4′-dihydroxybenzoyl)-2,4,6-trihydroxyphenylacetic acid [15].

Compound **6**, a pale-yellow powder. ESI-MS analysis provided an $[M + H]^+$ ion at m/z 355.10, which, combined with ^{13}C NMR data, established its molecular formula as $C_{16}H_{18}O_9$ (calculated for $C_{16}H_{19}O_9$, 355.10). The UV absorption maximum at 386 nm indicated an extended π-conjugation system. The presence of five olefinic protons was evident from the ^{1}H NMR spectrum (Fig. S11): signals consistent with a 1,3,4-trisubstituted benzene ring and an E-double bond were observed. The former was evidenced by three aromatic signals at δ_H 7.02 (H-6′), 6.87 (H-5′), and 7.08 (H-2′), while the latter was confirmed by two trans-coupled olefinic protons at δ_H 7.54 (H-7′) and 6.33 (H-8′). In the ^{13}C NMR spectrum (Fig. S12): δ_C 146.9 (C-4′), 146.1 (C-7′), 144.1 (C-3′), 126.9 (C-1′), 122.6 (C-6′), 116.1 (C-5′), 115.0 (C-8′), and 114.6 (C-2′), confirming a caffeyl moiety. Two carbonyl carbons at δ_C 181.2 (C-7) and 169.0 (C-9′) suggested the presence

of carboxyl and ester groups. Additionally, the aliphatic region showed signals at δ_C 40.5 (C-2) and 35.7 (C-6), along with four oxygenated carbon δ_C 76.0 (C-1), 73.5 (C-4), 72.8 (C-5), 66.9 (C-3), characteristic of a quinic acid skeleton. Based on comprehensive analysis of the spectroscopic data (Table 2) and comparison with literature data, compound **6** was identified as neochlorogenic acid [16].

Table 2: The ^{13}C NMR data of compounds **5**–**8** (δ in ppm).

No	5	6	7	8	No	5	6	7	8
1	108.1	76.0	76.6	76.0	1′	121.7	126.9	121.3	126.4
2	158.3	40.5	37.6	35.7	2′	117.9	114.6	114.7	130.4
3	101.4	66.9	71.4	72.9	3′	146.4	144.1	144.9	115.9
4	158.6	73.5	73.0	73.5	4′	152.4	146.9	148.9	158.1
5	102.1	72.8	71.2	66.9	5′	116.1	116.1	115.9	115.9
6	152.2	35.7	42.2	40.6	6′	124.4	122.6	125.3	130.4
7	30.7	181.2	177.2	181.4	7′	166.5	146.1	145.9	146.1
8	177.1	—	—	—	8′	—	115.0	114.3	114.5
					9′	—	169.0	167.1	168.1

Compound **5** tested in CD_3OD, compounds **6**, **8** tested in D_2O, compound **7** tested in DMSO, 100 MHz.

Compound **7** as a white powder exhibited the same molecular formula as compound **6**, $C_{16}H_{18}O_9$, which was established based on ESI-MS data, as evidenced by the $[M + Na]^+$ ion at m/z 377.08 (calculated for $C_{16}H_{18}O_9Na$, 377.08). A high degree of similarity was noted between the ^{1}H NMR spectra of compounds **7** and **6** (Figs. S11 and S13), indicating a shared identical carbon skeleton. However, careful analysis of their ^{13}C NMR spectra (Fig. S14) revealed slight chemical shift differences at C-3 ($\Delta\delta_C$ = 4.5 ppm), C-4 ($\Delta\delta_C$ = −0.5 ppm), C-2 ($\Delta\delta_C$ = −2.9 ppm), and C-6 ($\Delta\delta_C$ = 6.5 ppm). Given that compound **6** possesses multiple chiral centers, it was postulated that the differences between compounds **6** and **7** might arise from the configurational change at one or more chiral centers. By contrasting the spectroscopic data of compound **7** (Table 2) with those of chlorogenic acid [17], compound **7** was unambiguously identified as chlorogenic acid. Thus, compounds **6** and **7** were determined to be epimers, differing in configuration at the C-1, C-3, C-4 positions of the quinic acid moiety.

Compound **8**, acquired as white powder. The molecular formula $C_{16}H_{18}O_8$ was determined based on ESI-MS data, as evidenced by the $[M + H]^+$ ion at m/z 339.11 (calculated for $C_{16}H_{19}O_8$, 339.11). A detailed comparison of the ^{1}H and ^{13}C NMR spectra of compounds **8** and **6** revealed a high degree of similarity in their structures. However, a distinct additional olefinic proton was observed in compound **8**, and significant differences were noted in the downfield ^{13}C NMR signals was evident. Signals were showed in the ^{1}H NMR spectrum (Fig. S15) at δ_H 7.56 (2H, d, J = 8.5 Hz, H-2′/6′) and 6.92 (2H, d, J = 8.5 Hz, H-3′/5′), showing a typical AA'BB' coupling pattern characteristic of a 1,4-disubstituted benzene ring. These assignments were supported by corresponding ^{13}C NMR signals (Fig. S16) at δ_C 115.9 (C-3′/5′) and δ_C 130.4 (C-2′/6′). Excellent agreement was observed for the spectroscopic data of compound **8** (Table 2) in comparison with those of 3-O-p-coumaroylquinic acid from the literature, thus leading to the identification of compound **8** as 3-O-p-coumaroylquinic acid [18].

3.2 Cytotoxicity Assay

To exclude potential cytotoxicity-induced false positives in anti-inflammatory assays, compounds **1**–**8** were first evaluated for cytotoxicity using the CCK-8 assay (40 μM). As a positive control, Dex was utilized. It was found that treatment with compounds **1** and **2** reduced the viability of RAW264.7 cells to 51.06% and

44.91%, respectively (Fig. 2). In contrast, cells treated with compounds **3**–**8** maintained viability above 70%, comparable to the Dex group, which suggests negligible cytotoxicity.

This effect may be attributed to the ursane type skeleton common to both compounds **1** and **2**. The heightened hydrophobicity conferred by this structure leads to more severe cell membrane disruption, potentially explaining their stronger cytotoxicity. Therefore, compounds **3**–**8** were selected for further investigation of their anti-inflammatory activity.

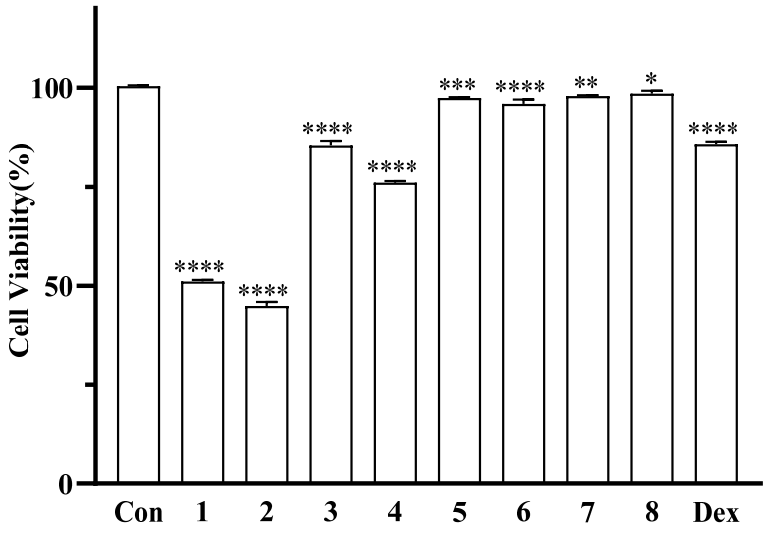

Figure 2: The cytotoxicity of compounds **1**–**8** on RAW264.7 cells at 40 μM. $^{*}p < 0.05$, $^{**}p < 0.01$, $^{***}p < 0.001$, $^{****}p < 0.0001$.

3.3 In Vitro Anti-Inflammatory Activity Assay

Based on the traditional use of *Prunus cerasifera* in treating inflammatory diseases, the anti-inflammatory activities of the isolated compounds were evaluated using an LPS-induced RAW264.7 cell model. According to the cytotoxicity results, the anti-inflammatory potential of compounds **3**–**8** was evaluated in RAW264.7 cells using LPS-induced inflammation model. As shown in Table 3, all tested compounds exhibited anti-inflammatory activity at varying degrees. Notably, compounds **6** and **7** displayed significantly higher anti-inflammatory activity (IC_{50} = 6.33 μM ± 0.18 μM and 8.06 μM ± 0.35 μM, respectively) than the positive control Dex (IC_{50} = 11.13 μM ± 0.43 μM).

This result can likely be attributed to their unique phenolic acid structures. Featuring a catechol group as a potent antioxidant core and multiple hydroxyl groups acting as hydrogen-bond donors, they achieve upstream suppression and multitarget regulation of inflammatory pathways such as NF-*k*B and NLRP3. Consequently, they effectively reduce the expression of key pro-inflammatory mediators while maintaining low cytotoxicity.

Table 3: Anti-inflammatory activity assay of compounds **3**–**8** and Dex.

Compounds	IC_{50} (μM)	Compounds	IC_{50} (μM)
3	14.57 ± 0.18	**7**	8.06 ± 0.35
4	16.52 ± 0.14	**8**	23.53 ± 0.51
5	14.87 ± 0.55	Dex	11.13 ± 0.43
6	6.33 ± 0.18		

3.4 In Vivo Anti-Inflammatory Activity Assay

To further investigate the anti-inflammatory activity of compounds **6** and **7** and their potential association with key pro-inflammatory factors, their effects on the production of IL-1β and IL-6 were examined in LPS-stimulated zebrafish using specific ELISA kits. Results of the anti-inflammatory activity of compounds **6** and **7** are summarized in Fig. 3. In LPS-challenged zebrafish larvae, compounds **6** and **7** exert anti-inflammatory effects primarily by modulating the pro-inflammatory cytokines IL-6 and IL-1β, and dose-dependently inhibit LPS-induced production of IL-1β and IL-6.

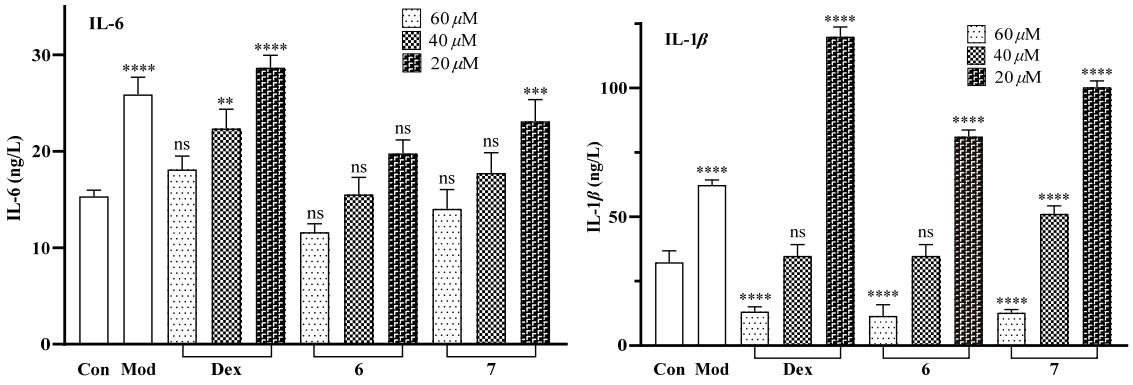

Figure 3: Inhibitory effects of compounds **6** and **7** on pro-inflammatory factors in zebrafish *in vivo*. ns: not significant, $^{**}p < 0.01$, $^{***}p < 0.001$, $^{****}p < 0.0001$.

4 Discussion

Several compounds isolated from the fruits of *Prunus cerasifera* Ehrh. were found to exhibit certain anti-inflammatory activity in both the inflammation model constructed using RAW 264.7 cells and the *in vivo* zebrafish experimental model. These findings confirmed previous reports on the chemical constituents and anti-inflammatory effects of *Prunus cerasifera* Ehrh. fruits [9,19,20], and the cytotoxicity and anti-inflammatory effects of the obtained compounds were similar to those of existing studies [21–23]. However, owing to the limited number of compounds isolated and identified from *Prunus cerasifera* Ehrh. fruits to date, whether the overall anti-inflammatory activity of *Prunus cerasifera* Ehrh. fruits is predominantly attributable to other classes of compounds, or whether it involves synergistic interactions among multiple compounds, remains insufficiently substantiated. Therefore, future studies should further expand the isolation and identification of active constituents from *Prunus cerasifera* Ehrh. fruits, thereby providing a more comprehensive elucidation of the material basis underlying their pharmacological effects.

In summary, this study innovatively clarifies the material basis for the anti-inflammatory action of *Prunus cerasifera* Ehrh. fruits and confirms the *in vivo* activity of its monomeric compounds using a zebrafish model that is physiologically more relevant to humans. This work establishes a theoretical foundation for developing this resource into functional foods or natural drug leads.

5 Conclusion

This study isolated eight compounds from *Prunus cerasifera* Ehrh. fruits, including four triterpenoids (**1**–**4**), a phenylethanoid glycoside (**5**) and three phenolic acids (**6**–**8**). These compounds have not been previously isolated from this fruit, with the triterpenoids being the first of their kind reported in the fruits. Notably, compounds **6** and **7** showed potent anti-inflammatory activity in LPS-induced RAW264.7 cells, with IC_{50} values of 6.33 μM ± 0.18 μM and 8.06 μM ± 0.35 μM, respectively, outperforming the positive control

Dex (IC_{50} = 11.13 μM ± 0.43 μM). Furthermore, *in vivo* anti-inflammatory assays in zebrafish further showed that the anti-inflammatory effects of compounds **6** and **7** are primarily mediated through the regulation of pro-inflammatory factors IL-6 and IL-1β. This research expands the scope of natural product chemistry related to *Prunus cerasifera* Ehrh. fruits, clarifies the chemical structures of some of its active components, and provides insights into its potential anti-inflammatory mechanisms through bioactivity evaluation.

Acknowledgement: Not applicable.

Funding Statement: This project was funded by Natural Science Foundation of Xinjiang Uygur Autonomous Region (2022D01C455), College Student Innovation and Entrepreneurship Training Program (202410764010).

Author Contributions: Haofan Lv was responsible for the isolation and purification of the fractions and authored the initial draft; Qihang Zhang and Yufan He performed the compounds confirmation and structural explanation; Wuwei Xin conducted bioactivity testing; Wei Liu and Chunpeng Wan oversaw the experimental design and manuscript revision. All authors reviewed and approved the final version of the manuscript.

Availability of Data and Materials: The authors confirm that the data supporting the findings of this study are available within the article and its Supplementary Materials.

Ethics Approval: Not applicable.

Conflicts of Interest: The authors declare no conflicts of interest.

Supplementary Materials: The supplementary material is available online at https://www.techscience.com/doi/10.32604/phyton.2026.076015/s1.

References

1. Pezone A, Olivieri F, Napoli MV, Procopio A, Avvedimento EV, Gabrielli A. Inflammation and DNA damage: cause, effect or both. Nat Rev Rheumatol. 2023;19(4):200–11. [CrossRef].
2. Patel S. Inflammasomes, the cardinal pathology mediators are activated by pathogens, allergens and mutagens: a critical review with focus on NLRP3. Biomed Pharmacother. 2017;92:819–25. [CrossRef].
3. Almascati Y, Alhumaiqani A, Wen B, Alarayedh T. Ischemic colitis induced by concurrent non-steroidal anti-inflammatory drug (NSAID) and corticosteroid use for back pain. Cureus. 2025;17(8):e90548. [CrossRef].
4. Song W, Qin ST, Fang FX, Gao ZJ, Liang DD, Liu LL, et al. Isolation and purification of condensed tannin from the leaves and branches of *Prunus cerasifera* and its structure and bioactivities. Appl Biochem Biotechnol. 2018;185(2):464–75. [CrossRef].
5. Wang Y, Chen X, Zhang Y, Chen X. Antioxidant activities and major anthocyanins of Myrobalan plum (*Prunus cerasifera* Ehrh.). J Food Sci. 2012;77(4):C388–93. [CrossRef].
6. Chen FF, Sang J, Zhang Y, Sang J. Development of a green two-dimensional HPLC-DAD/ESI-MS method for the determination of anthocyanins from *Prunus cerasifera* var. atropurpurea leaf and improvement of their stability in energy drinks. Int J Food Sci Technol. 2018;53(6):1494–502. [CrossRef].
7. Cantín CM, Moreno MA, Gogorcena Y. Evaluation of the antioxidant capacity, phenolic compounds, and vitamin C content of different peach and nectarine [*Prunus persica* (L.) Batsch] breeding progenies. J Agric Food Chem. 2009;57(11):4586–92. [CrossRef].
8. Hooshmand S, Kumar A, Zhang JY, Johnson SA, Chai SC, Arjmandi BH. Evidence for anti-inflammatory and antioxidative properties of dried plum polyphenols in macrophage RAW 264.7 cells. Food Funct. 2015;6(5):1719–25. [CrossRef].
9. Duan X, Li J, Cui J, Wen H, Xin X, Aisa HA. A network pharmacology strategy combined with *in vitro* experiments to investigate the potential anti-inflammatory mechanism of *Prunus cerasifera* Ehrhart. J Food Biochem. 2022;46(12):e14396. [CrossRef].

10. Yu YH, Feng YP, Liu W, Yuan T. Diverse triterpenoids from mastic produced by *Pistacia lentiscus* and their anti-inflammatory activities. Chem Biodivers. 2022;19(3):e202101012. [CrossRef].
11. Zeng HT, Yu YH, Zeng X, Li MM, Li X, Xu SS, et al. Anti-inflammatory dimeric benzophenones from an endophytic pleosporales species. J Nat Prod. 2022;85(1):162–8. [CrossRef].
12. Li X, Yang Z, Yu D, Zhang Y, Shen Z, Meng Y, et al. Study on the chemical composition, zebrafish toxicity and anti-inflammatory activity of *Ecklonia kurome*. J Ethnopharmacol. 2025;352:120171. [CrossRef].
13. Seebacher W, Simic N, Weis R, Saf R, Kunert O. Complete assignments of ^{1}H and ^{13}C NMR resonances of oleanolic acid, 18α-oleanolic acid, ursolic acid and their 11-oxo derivatives. Magn Reson Chem. 2003;41(8):636–8. [CrossRef].
14. Saidi I, El Ayeb-Zakhama A, Harzallah-Skhiri F, Ben Jannet H. Phytotoxicity of pentacyclic triterpene acids from *Citharexylum spinosum* L. to radish, lettuce and canary grass. Allelopath J. 2018;45(2):243–54. [CrossRef].
15. Hillenbrand M, Zapp J, Becker H. Depsides from the petals of *Papaver rhoeas*. Planta Med. 2004;70(4):380–2. [CrossRef].
16. Kim TH. Chlorogenic acid isomers from Sorbus commixta of Ulleung island origin and their inhibitory effects against advanced glycation end product (AGE) formation and radical scavenging activity. J Korean Soc Food Sci Nutr. 2016;45(8):1208–13. [CrossRef].
17. Delnavazi MR, Hadjiakhoondi A, Delazar A, Ajani Y, Yassa N. *Azerosides A* and *B*: Two new phloroacetophenone glycosides from the roots of *Dorema glabrum* Fisch. & C. A. Mey. Med Chem Res. 2015;24(2):787–96. [CrossRef].
18. da Silva Pinto L, de Souza FHD, Nascimento IR, Lopes LMX. Phenylpropanoids from *Paspalum atratum* (poaceae). Biochem Syst Ecol. 2015;63:68–71. [CrossRef].
19. Huang H. Comparative investigation of the chemical composition and the water permeability of fruit and leaf cuticles [dissertation]. Würzburg, Germany: Universität Würzburg; 2018. 183 p.
20. Luo SB, Liu W, Xie X, Feng YP, Peng CY, Zhang L. Antioxidant and hypoglycemic activities of purple *Prunus cerasifera* Ehrh extracts and identification of chemical constituents. Food Ferment Ind. 2024;50(19):191–200. [CrossRef].
21. Wang SH, Jiang H, Yu H, Liu SW, Li MH, Wang LY, et al. Effects of ursolic acid at different concentrations on proliferation and differentiation of osteoclasts and their significances. J Jilin Univ Med Ed. 2017;43(2):236–40. [CrossRef].
22. Ma B, Zhang H, Wang Y, Zhao A, Zhu Z, Bao X, et al. Corosolic acid, a natural triterpenoid, induces ER stress-dependent apoptosis in human castration resistant prostate cancer cells via activation of IRE-1/JNK, PERK/CHOP and TRIB3. J Exp Clin Cancer Res. 2018;37(1):210. [CrossRef].
23. Zhou J, Xue C, Zhang Q, Chen SY, Chen Y, Huang J, et al. Establishment of a method determining the contents of seven anti-inflammatory active components of the Miao medicine in *ula* cappa in Raw 264.7 cells. J Jiangsu Univ Med Ed. 2022;32(6):524–31. [CrossRef].